

Article

Modeling of Tensile Test Results for Low Alloy Steels by Linear Regression and Genetic Programming Taking into Account the Non-Metallic Inclusions

Miha Kovačič^{1,2,3,*} and Uroš Župerl⁴

¹ ŠTORE STEEL, d.o.o., Research and Development, 3220 Štore, Slovenia

² Laboratory for Fluid Dynamics and Thermodynamics, Faculty of Mechanical Engineering, University of Ljubljana, 1000 Ljubljana, Slovenia

³ College of Industrial Engineering, 3000 Celje, Slovenia

⁴ Faculty of Mechanical Engineering, University of Maribor, 2000 Maribor, Slovenia

* Correspondence: miha.kovacic@store-steel.si

Abstract: Štore Steel Ltd. is one of the biggest flat spring steel producers in Europe. The main motive for this study was to study the influences of non-metallic inclusions on mechanical properties obtained by tensile testing. From January 2016 to December 2021, all available tensile strength data (472 cases–472 test pieces) of 17 low alloy steel grades, which were ordered and used by the final user in rolled condition, were gathered. Based on the geometry of rolled bars, selected chemical composition, and average size of worst fields non-metallic inclusions (sulfur, silicate, aluminium and globular oxides), determined based on ASTM E45, several models for tensile strength, yield strength, percentage elongation, and percentage reduction area were obtained using linear regression and genetic programming. Based on modeling results in the period from January 2022 to April 2022, five successively cast batches of 30MnVS6 were produced with a statistically significant reduction of content of silicon (*t*-test, $p < 0.05$). The content of silicate type of inclusions, yield, and tensile strength also changed statistically significantly (*t*-test, $p < 0.05$). The average yield and tensile strength increased from 458.5 MPa to 525.4 MPa and from 672.7 MPa to 754.0 MPa, respectively. It is necessary to emphasize that there were no statistically significant changes in other monitored parameters.

Keywords: mechanical properties; tensile test; tensile strength; yield strength; percentage elongation; percentage reduction area; low alloy steel; modeling; linear regression; genetic programming; industrial study; steel making; optimization

Citation: Kovačič, M.; Župerl, U. Modeling of Tensile Test Results for Low Alloy Steels by Linear Regression and Genetic Programming Taking into Account the Non-Metallic Inclusions. *Metals* **2022**, *12*, 1343. <https://doi.org/10.3390/met12081343>

Academic Editor: Cristiano Fragassa

Received: 30 June 2022

Accepted: 9 August 2022

Published: 12 August 2022

Publisher's Note: MDPI stays neutral with regard to jurisdictional claims in published maps and institutional affiliations.



Copyright: © 2022 by the authors. Licensee MDPI, Basel, Switzerland. This article is an open access article distributed under the terms and conditions of the Creative Commons Attribution (CC BY) license (<https://creativecommons.org/licenses/by/4.0/>).

1. Introduction

The tensile testing of metallic materials, as one of the most important methods of testing, which is usually performed at room temperature (i.e., between 10 °C and 35 °C), includes the following steps:

- taking of samples,
- preparation of test pieces (usually machining),
- pulling the test piece by tensile force until the breakage,
- obtaining mechanical properties based on measurements and calculations (e.g., tensile strength, yield strength, percentage elongation, percentage reduction area).

Mechanical properties obtained by tensile testing mostly depend on:

- material chemical composition,
- material macrostructure (e.g., segregations, sheets and strips) and microstructure (e.g., grain size and morphology, content of microstructures),

- sampling (location and orientation of test pieces),
- preparation of test pieces (machining, heat treatment),
- tensile test performance (e.g., equipment, testing speed).

On the other hand, non-metallic inclusions should also not be neglected while their presence as foreign substances can disrupt the existing structure as well as cause cracks and fatigue failure.

Below, a few studies are presented where, beside the chemical composition, influences of non-metallic inclusions on mechanical properties of steel were also elaborated. They are generally limited to individual steel grade [1–17] and individual type of inclusions [2,5–17] especially based on rare earth elements [5,11,12,15–17]. At the same time, attention is paid to grain morphology, size [12,17,18], microstructure [7,11,12], and heat treatment [1,12,13,18]. Only a few industrial studies are available [9,15].

Qiu and coauthors [1] used two ferritic/martensitic steel grades where Y, Ti, and Zr were transformed into steels through vacuum induction melting. Steel was additionally tempered at 650 °C. Y, Ti, and especially Zr based particles were formed. It was shown that the presence Zr-rich inclusions caused a reduction in mechanical properties. A balance between the formation of inclusions and the tempering temperature could support the improvement of strength and impact toughness.

In the paper [18], the influence of boron and niobium on the microstructure and consequent changes in the mechanical properties of hot-rolled low-carbon bainite steel was investigated. Additionally, hardenability and phase transformation were analyzed. For microstructure analysis and non-metallic inclusion contents, laser scanning confocal microscopy and field emission scanning electron microscopy were used. It was found that the boron does not influence hardness, yield, or tensile strength. The addition of boron generally reduced the impact toughness. The authors explain the outcomes in terms of micro-cleanliness, slight microstructural changes, grain size, and precipitation of coarse $(Fe,Cr)_{23}(B,C)_6$.

Gong and coauthors [2] studied the addition of Mg to Cr12Mo1V1 steel to observe changes in the composition, morphology, size, and distribution of non-metallic inclusions. Added Mg formed $MgO \cdot Al_2O_3$ and MgO inclusions as well as MnS–MgS precipitates. It was also found that due to the presence of Mg, the Mg-containing inclusions increase, consequently the density of inclusions decreases, which result in efficient inclusion removal. In addition, strength and plasticity are improved.

The effect of the content of non-metallic inclusions on the impact toughness of 32 CDV 13 steel is analyzed in the article [3]. Based on the fractography of the Charpy impact test samples, it was found that the impact toughness increases with decreasing content of non-metallic inclusions. The significant influence was attributed to micro-cracking at the grow of the inclusion-nucleated voids. Moreover, numerical simulations using COMSOL Multiphysics software were used to calculate the concentrated stresses of the steel matrix around the non-metallic inclusions. Calculated stress concentrations are higher at sulfide inclusions than oxide inclusions.

Similarly, Liu et al. [4] investigated the effect of the size and distribution of non-metal inclusions on mechanical properties of low activation martensitic steel. By optical and scanning electron microscope, the aluminium based non-metallic inclusions content was determined. The aluminium inclusions content was reduced using electroslag remelting. Accordingly, the mechanical properties were improved.

In the paper [5], cerium addition to interstitial free steel was studied in order to analyze the influences on mechanical properties. Cerium based inclusions forms Al_2O_3 and TiN- Al_2TiO_5 - Al_2O_3 to Ce_2O_3 , Ce_2O_2S , $CeAlO_3$, TiN- Al_2TiO_5 - Ce_2O_3 , and TiN- Al_2TiO_5 - Ce_2O_2S composite inclusions with various thermal coefficients and hardness (i.e., brittleness). It can be concluded that due to small differences between thermal coefficients and the hardness of cerium-based inclusions and iron matrix, higher mechanical properties were achieved.

Wu and coauthors [6] studied the influence of MnS inclusions morphology and spatial distribution on elongation, reduction area, yield and tensile strength. In the experiment, hot rolled bars made from steel containing 0.03% of sulphur were used. The variations of elongation and reduction area increased in the transverse direction while the tensile strength and yield strength remained practically unchanged. The MnS inclusions were classified into three types: parallel elongated MnS inclusions, densely distributed tiny MnS inclusions, and spindle-shaped MnS inclusions. Based on their parameters and probe orientation reduction area linear regression was used for reduction area prediction. Based on linear regression results densely distributed tiny MnS inclusions should be avoided.

Similarly, Lu et al. [9] investigated transverse tensile properties of hot rolled bars from two commercial steel grades while varying Ca, Al, Mg, and Mn contents in steel. Consequently, inclusions with different morphology and distribution formed. It was found that due to agmination of MnS inclusions, the transverse ductility worsened due to higher stress concentrations.

Qiu et al. [7] investigated the effect of Zr addition on the inclusion formation, microstructure, tensile properties, and impact toughness of the low activation martensitic steel. The addition of Zr varied from 0.01% to 0.11%. Scanning electron microscope was used for examination of Zr-based inclusions and Zr-based precipitates. It was found out that Zr content deteriorates the mechanical properties. Accordingly, the highest yield and tensile strength values were obtained at 0.01% of Zr where Zr_3V_3C carbides were precipitated.

Zirconium addition was also investigated using cast heavy section steel [8]. Optical and scanning electron microscopes have been used for examination of inclusions. However, compared with the research mentioned above, the mechanical properties (Tensile and Charpy V-notch impact test) improved due to the addition of Zr. The examinations also show that the Zr addition modifies MnS inclusions.

Similarly, the effect of yttrium low activation martensitic steel was investigated [12]. By adding yttrium, AC3 temperature was increased. Afterward, the tempering process was optimized in order to control carbide precipitations. It was found that based on precipitate dispersion, carbides were smaller. On the other hand, the coarsening of martensite laths and coarsening of grains occurred after tempering. This effect decreased after quenching the low activation martensitic steel twice.

Gupta et al. [19] studied the effect of inclusions on the forming operation of steel sheets using two-dimensional finite element analysis. The focus was to understand the void formation and matrix inclusion interactions. Based on the finite element method and properties of the inclusions, the properties of steel matrix were predicted. Accordingly, the failures during hot rolling could also be determined.

The authors in [11] analysed the influences on cerium addition on carbides formation and mechanical properties of cast high grade knives steel. The size and morphology of carbides and mechanical properties were studied using optical microscopy, scanning electron microscopy, and X-ray diffraction. It was found that cerium refines cast microstructure, as well as changes the type of inclusions and carbide morphology, where rod-shaped carbides turn into lamellae. It can be concluded that cerium acts as nucleator of carbides, reducing the size and distribution of carbides in cast steel and consequently improving mechanical properties.

In the research [14], the influence of TiN inclusions on delayed cracking after flame cutting of high strength, wear resistant steel was studied. Optical microscopy, scanning electron microscopy, X-ray diffraction, transmission electron microscopy, and electron backscattered diffractometry were used. It was found out that the delayed cracking occurred from segregations during solidification and also can be attributed to micro TiN inclusions.

In their industrial study, Jonšta and coauthors [15] analyzed cerium addition to 42CrMo4 steel, which was used for forging. Loss of cerium during melting and due to reoxidation and also mechanical properties were monitored. The expected microstructure refinement and improved mechanical properties were not achieved. Moreover, the loss of

cerium during steelmaking reached 50%. The locally segregated cerium inclusions caused initiation of cracks. Furthermore, several types of cerium based inclusions were detected in forged bars.

Similarly, the effect of cerium addition on the grain size, tensile, and impact properties of LDX2101 duplex stainless steel was investigated [16]. For inclusion analyses, optical and scanning electron microscopes were used. The results show the formation of different types, sizes, and distributions of inclusions affecting the grain size and consequently mechanical properties. With the addition of cerium, the energy absorbed during the impact test, tensile strength, yield strength, and elongation improved.

In this industrial study, we covered all available tensile strength data (472 cases–472 test pieces) of 17 steel grades which were ordered and used by the final user in rolled condition. The rolled bars were produced from January 2016 to December 2021 in Štore Steel Ltd., which is one of the biggest flat spring steel producers in Europe. The samples were taken from serial production, with test pieces machined using the same equipment by the same group of machine operators and the tensile testing performed by the same operator and using the same tensile test machine. The main motive was to see the influence of non-metallic inclusions on mechanical properties obtained by tensile testing. Based on the geometry of rolled bars, selected chemical composition, and average size of worst field non-metallic inclusions (sulfur, silicate, aluminium and globular oxides), several models for tensile strength, yield strength, percentage elongation, and percentage reduction area were obtained using linear regression and genetic programming. Based on developed models, the influences of individual parameters were also calculated. The modeling results were validated with improved yield and tensile strength of 30MnVS6 produced in 2022.

2. Materials and Methods

Production in Štore Steel Ltd. (Štore, Slovenia) steel plant consists of melting of the scrap using an electric arc furnace, tapping, ladle treatment (i.e., secondary metallurgy), and continuous casting of the 180 mm × 180 mm billets. The cast billets are reheated and rolled in the rolling plant using three rolling stands. First, two rolling stands are duo reversible stands (800 mm and 650 mm diameter rolls) and the last continuous rolling line (460 mm diameter rolls) has 6 horizontal and 4 vertical stands.

In this industrial study, we covered all available tensile strength data (472 cases–472 test pieces) of 17 steel grades which were ordered and used by the final user in rolled condition. The rolled bars were produced from January 2016 to December 2021 in Štore Steel Ltd. which is one of the biggest flat spring steel producers in Europe. The samples were taken from serial production.

According to ISO 14,284 (Steel and iron-sampling and preparation of samples for the determination of chemical composition) immersion probes are inserted manually into the melt in tundish using a lance attached directly to the probe assembly. The chemical composition of obtained disc samples (using immersion probes) was determined according to ASTM E1019 (carbon and sulfur) ASTM E415 (for all other elements). For chemical composition determination ELTRA ONHp analyzer (Eltra GmbH, Haan, Germany), ELTRA CSi analyzer (Eltra GmbH, Haan, Germany) (according to ASTM E1019), and SPECTRO-LAB LAVMC12A (SPECTRO Analytical Instruments GmbH, Kleve, Germany) (according to ASTM E415) were used.

Non-metallic inclusion content was determined according to ASTM E45. According to standard at least six representative samples per lot (i.e., quantity of steel from the same batch and the same geometry) should be examined using a microscope. The minimum polished surface area of a specimen for the microscopic determination of inclusion content is 160 mm². Based on standard, the inclusions are classified into four categories (types) based on their morphology and also on two subcategories based on their width or diameter. Categories are:

- A: sulfide type,
- B: alumina type,
- C: silicate type and
- D: globular oxide type.

All can be subcategorized into heavy and thin describing their thickness. In this study, we considered only the size of the inclusions regardless of thickness. According to standard severity numbers are used representing the size of inclusions. Moreover, method A—worst fields was used. Using method A, all the severity numbers, related with size of inclusions, at the worst field of the samples (at least six representative samples) are averaged.

Samples were obtained from rolled bars with diameter from 18 mm to 110 mm and flat bars with thickness from 8 mm to 73 mm and width from 45 mm to 200 mm from the middle billet of the rolling lot. Preparation of samples and test pieces was conducted according to ISO 377 (Steel and steel products—Location and preparation of samples and test pieces for mechanical testing).

Test probes were made according to ISO 527-2 type 1B.

The tensile testing was performed using the Messphysik Beta 300 tensile test machine (MESSPHYSIK MATERIALS TESTING GmbH, Fürstenfeld, Austria) (Figure 1) according to ISO 6892-1.

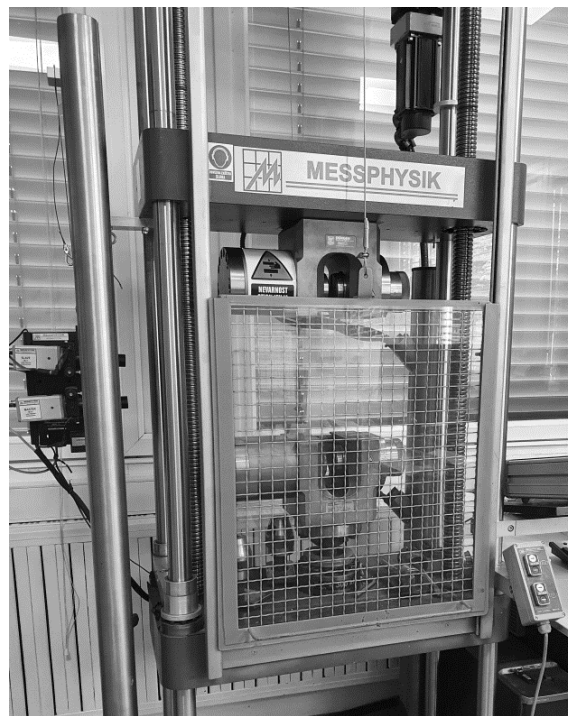


Figure 1. Messphysik Beta 300 tensile test machine.

Following parameters were collected within the period from January 2016 to December 2021 in Štore Steel Ltd. for 472 cases—472 test pieces of 17 steel grades (Table 1):

- Carbon (Carbon), silicon (Si), manganese (Mn), silicon (Si), phosphorus (P), sulfur (S), chromium (Cr), molybdenum (Mo), nickel (Ni) and aluminium (Al) content in weight%.
- Severity number for sulfide type of inclusions (A) determined according to standard ASTM E45, method A. Based on mentioned standard the inclusions can subcategorized into heavy and thin describing their thickness. In the research only maximal severity number was used for categorization of inclusions size.

- Severity number for alumina type of inclusions (B) determined according to standard ASTM E45, method A.
- Severity number for silicate type of inclusions (C) determined according to standard ASTM E45, method A.
- Severity number for globular type of inclusions (D) determined according to standard ASTM E45, method A.
- Tensile (Rm) and yield (Rp0.2) strength, percentage elongation (Elongation) and reduction area (Reduction).

The chemical composition (average and standard deviation) of steel grades used in the research are gathered in the Table 1.

Table 1. The chemical composition (average and standard deviation) of steel grades used in the research.

| Steel Grade | Number of Cases | wt % C | | wt % Si | | wt % Mn | | wt % P | | wt % S | | wt % Cr | | wt % Mo | | wt % Ni | | wt % Al | |
|-------------|-----------------|--------|-------|---------|-------|---------|-------|--------|-------|--------|-------|---------|-------|---------|-------|---------|-------|---------|-------|
| | | Av | Std | Av | Std | Av | Std | Av | Std | Av | Std | Av | Std | Av | Std | Av | Std | Av | Std |
| 15CrNi6 | 2 | 0.170 | 0.000 | 0.310 | 0.000 | 0.550 | 0.000 | 0.009 | 0.000 | 0.008 | 0.000 | 1.570 | 0.000 | 0.080 | 0.000 | 1.520 | 0.000 | 0.007 | 0.000 |
| 16MnCr5 | 1 | 0.160 | / | 0.280 | / | 1.100 | / | 0.012 | / | 0.021 | / | 0.890 | / | 0.060 | / | 0.150 | / | 0.018 | / |
| 16MnCrS5 | 13 | 0.171 | 0.014 | 0.268 | 0.006 | 1.115 | 0.052 | 0.011 | 0.001 | 0.025 | 0.004 | 0.975 | 0.056 | 0.033 | 0.010 | 0.107 | 0.026 | 0.018 | 0.002 |
| 20CrMo5 | 15 | 0.199 | 0.003 | 0.237 | 0.009 | 1.030 | 0.004 | 0.014 | 0.001 | 0.021 | 0.001 | 1.180 | 0.008 | 0.210 | 0.004 | 0.201 | 0.031 | 0.016 | 0.000 |
| 20MnCr5 | 31 | 0.176 | 0.008 | 0.288 | 0.012 | 0.903 | 0.014 | 0.013 | 0.001 | 0.007 | 0.001 | 1.065 | 0.008 | 0.021 | 0.003 | 0.075 | 0.008 | 0.017 | 0.002 |
| 20MnCrS5 | 7 | 0.191 | 0.004 | 0.240 | 0.000 | 1.280 | 0.026 | 0.014 | 0.001 | 0.023 | 0.000 | 1.177 | 0.008 | 0.040 | 0.000 | 0.123 | 0.008 | 0.019 | 0.000 |
| 20MnV6 | 31 | 0.170 | 0.000 | 0.157 | 0.071 | 1.546 | 0.015 | 0.012 | 0.002 | 0.023 | 0.001 | 0.194 | 0.015 | 0.034 | 0.015 | 0.170 | 0.000 | 0.022 | 0.003 |
| 28MnCrB7 | 10 | 0.288 | 0.008 | 0.158 | 0.006 | 1.260 | 0.028 | 0.013 | 0.004 | 0.009 | 0.003 | 0.397 | 0.015 | 0.047 | 0.013 | 0.133 | 0.022 | 0.018 | 0.001 |
| 30MnVS6 | 60 | 0.287 | 0.009 | 0.606 | 0.028 | 1.429 | 0.019 | 0.012 | 0.002 | 0.029 | 0.004 | 0.166 | 0.028 | 0.029 | 0.006 | 0.082 | 0.021 | 0.014 | 0.002 |
| 38MnVS6 | 5 | 0.372 | 0.004 | 0.530 | 0.000 | 1.298 | 0.004 | 0.012 | 0.002 | 0.047 | 0.004 | 0.132 | 0.018 | 0.028 | 0.004 | 0.082 | 0.018 | 0.010 | 0.001 |
| C22 | 14 | 0.167 | 0.009 | 0.096 | 0.008 | 0.318 | 0.006 | 0.008 | 0.002 | 0.006 | 0.002 | 0.121 | 0.026 | 0.021 | 0.004 | 0.074 | 0.025 | 0.023 | 0.004 |
| C35S | 3 | 0.390 | 0.000 | 0.270 | 0.000 | 0.660 | 0.000 | 0.013 | 0.000 | 0.024 | 0.000 | 0.200 | 0.000 | 0.030 | 0.000 | 0.080 | 0.000 | 0.021 | 0.000 |
| C45 | 14 | 0.460 | 0.004 | 0.255 | 0.014 | 0.631 | 0.003 | 0.011 | 0.001 | 0.026 | 0.004 | 0.239 | 0.029 | 0.055 | 0.013 | 0.144 | 0.015 | 0.019 | 0.001 |
| C45S | 33 | 0.452 | 0.004 | 0.291 | 0.020 | 0.628 | 0.004 | 0.010 | 0.001 | 0.026 | 0.002 | 0.182 | 0.004 | 0.026 | 0.012 | 0.088 | 0.017 | 0.021 | 0.004 |
| C60S | 110 | 0.583 | 0.005 | 0.241 | 0.024 | 0.712 | 0.014 | 0.010 | 0.002 | 0.027 | 0.002 | 0.126 | 0.021 | 0.022 | 0.004 | 0.081 | 0.019 | 0.019 | 0.004 |
| P460NH | 31 | 0.185 | 0.006 | 0.094 | 0.028 | 1.554 | 0.034 | 0.011 | 0.002 | 0.013 | 0.001 | 0.126 | 0.008 | 0.027 | 0.010 | 0.178 | 0.008 | 0.021 | 0.001 |
| S355J2 | 92 | 0.178 | 0.016 | 0.317 | 0.106 | 1.316 | 0.080 | 0.010 | 0.002 | 0.007 | 0.002 | 0.137 | 0.041 | 0.028 | 0.005 | 0.078 | 0.015 | 0.027 | 0.002 |

Gathered tensile, yield strength, percentage elongation, and reduction area data are presented in Table 2.

Table 2. The tensile, yield strength, percentage elongation and reduction area (average and standard deviation).

| Steel Grade | Rm [MPa] | | Rp0.2 [MPa] | | A [%] | | Z [%] | |
|-------------|----------|--------|-------------|--------|-------|------|-------|-------|
| | Av | Std | Av | Std | Av | Std | Av | Std |
| 15CrNi6 | 998.50 | 2.12 | 623.50 | 28.99 | 9.05 | 0.21 | 26.05 | 3.46 |
| 16MnCr5 | 605.00 | / | 364.00 | / | 11.00 | / | 25.00 | / |
| 16MnCrS5 | 559.54 | 69.67 | 370.23 | 60.73 | 19.40 | 3.57 | 49.66 | 8.47 |
| 20CrMo5 | 684.80 | 137.10 | 451.00 | 110.54 | 13.46 | 5.12 | 35.41 | 14.49 |
| 20MnCr5 | 653.29 | 75.79 | 453.13 | 58.35 | 17.55 | 3.53 | 50.83 | 16.55 |
| 20MnCrS5 | 685.00 | 119.56 | 435.43 | 68.28 | 15.99 | 4.29 | 48.43 | 15.00 |
| 20MnV6 | 709.74 | 125.16 | 474.39 | 90.46 | 15.79 | 4.84 | 40.31 | 11.56 |
| 28MnCrB7 | 661.20 | 103.85 | 416.60 | 83.10 | 17.00 | 2.96 | 46.22 | 11.88 |
| 30MnVS6 | 672.72 | 112.95 | 457.32 | 87.60 | 17.54 | 4.26 | 44.77 | 10.74 |
| 38MnVS6 | 684.40 | 59.51 | 465.00 | 59.47 | 13.98 | 2.23 | 37.38 | 9.81 |
| C22 | 700.86 | 200.85 | 470.07 | 142.41 | 16.38 | 7.64 | 39.09 | 14.59 |
| C35S | 633.00 | 52.14 | 404.67 | 24.54 | 18.40 | 3.86 | 45.93 | 16.17 |
| C45 | 651.21 | 118.67 | 400.86 | 75.50 | 17.95 | 4.73 | 44.66 | 15.70 |
| C45S | 644.18 | 162.35 | 437.12 | 126.09 | 16.92 | 4.97 | 45.07 | 13.11 |
| C60S | 665.55 | 134.29 | 432.13 | 86.73 | 16.46 | 4.54 | 43.02 | 13.58 |
| P460NH | 654.00 | 72.68 | 457.61 | 70.27 | 16.36 | 3.19 | 47.82 | 10.66 |
| S355J2 | 644.28 | 109.22 | 434.92 | 86.15 | 17.75 | 5.00 | 45.14 | 13.52 |

3. Modeling of Tensile, Yield Strength, Percentage Elongation and Reduction Area

On the basis of the collected data, the prediction of mechanical properties was conducted using linear regression and genetic programming. For the fitness function, the average relative deviation between predicted and experimental data was selected. It is defined as:

$$\Delta = \frac{\sum_{i=1}^n \frac{|Q_i - Q'_i|}{Q_i}}{n} \quad (1)$$

where n is the size of the monitored data and Q_i and Q'_i are the actual and the predicted mechanical property, respectively. For prediction of mechanical properties linear regression and genetic programming were used.

3.1. Modeling of Tensile, Yield Strength, Percentage Elongation and Reduction Area Using Linear Regression

The next model significantly predicts the tensile strength ($p < 0.05$, ANOVA) and that only 9.13% of total variances can be explained by independent variables variances (R-square). Significantly influential parameters ($p > 0.05$) are only chromium (Cr) and aluminium (Al) content.

$$\begin{aligned} R_m = & 0.36 \cdot WIDTH - 1.19 \cdot THICKNESS - 61.55 \cdot Carbon - 17.14 \cdot Si - 20.57 \cdot Mn \\ & - 3964.00 \cdot P - 1366.57 \cdot S - 63.01 \cdot Cr + 162.26 \cdot Mo - 72.24 \cdot Ni \\ & - 4137.51 \cdot Al + 30.79 \cdot A - 13.31 \cdot B - 262.22 \cdot C + 4.79 \cdot D \\ & + 782.93 \end{aligned} \quad (2)$$

The average relative deviation from experimental data is 14.78%.

In addition, the influences of individual parameters on the tensile strength while separately changing individual parameter within the individual parameter range were calculated (Figure 2). It is possible to conclude that according to linear regression results, the most influential are silicate type inclusions (C).

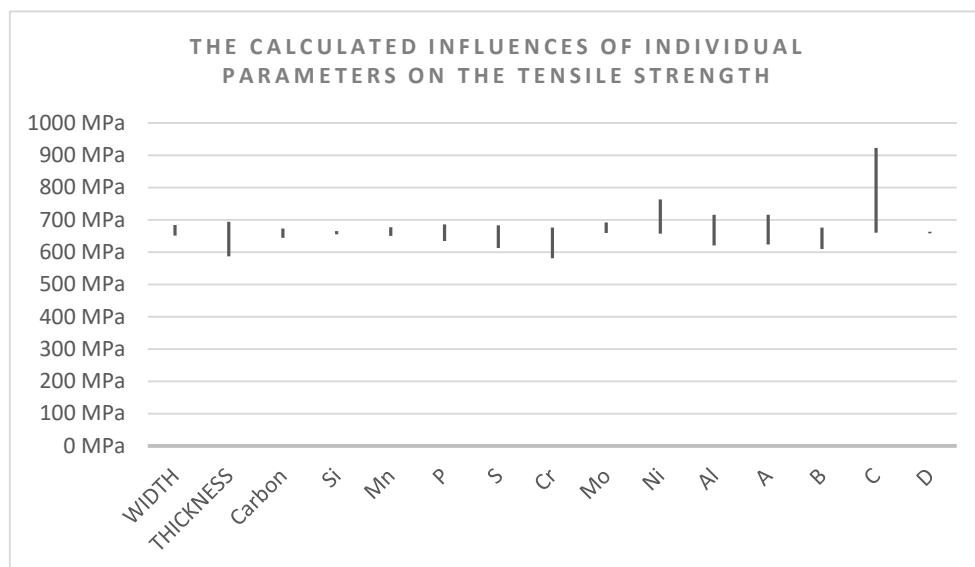


Figure 2. The calculated influences of individual parameters on the tensile strength while separately changing individual parameter within the individual parameter range.

The next model significantly predicts the yield strength ($p < 0.05$, ANOVA) but only 7.15% of total variances can be explained by independent variables variances (R-square). Significantly influential parameters ($p > 0.05$) are hot rolled bar width (WIDTH) and thickness (THICKNESS) and chromium content (Cr).

$$\begin{aligned}
 R_{p0.2} = & 1.90 \cdot WIDTH - 2.37 \cdot THICKNESS - 79.04 \cdot Carbon - 11.58 \cdot Si - 6.31 \cdot Mn \\
 & + 2463.53 \cdot P - 552.76 \cdot S + 55.44 \cdot Cr + 119.89 \cdot Mo + 47.64 \cdot Ni \\
 & - 2211.32 \cdot Al + 16.89 \cdot A - 5.43 \cdot B - 156.01 \cdot C + 1.05 \cdot D \\
 & + 509.09
 \end{aligned} \quad (3)$$

The average relative deviation from experimental data is 16.02%.

Moreover, the influences of individual parameters on the yield strength while separately changing individual parameter within the individual parameter range were calculated (Figure 3). It is possible to conclude that according to linear regression results the most influential are silicate type of inclusions (C).

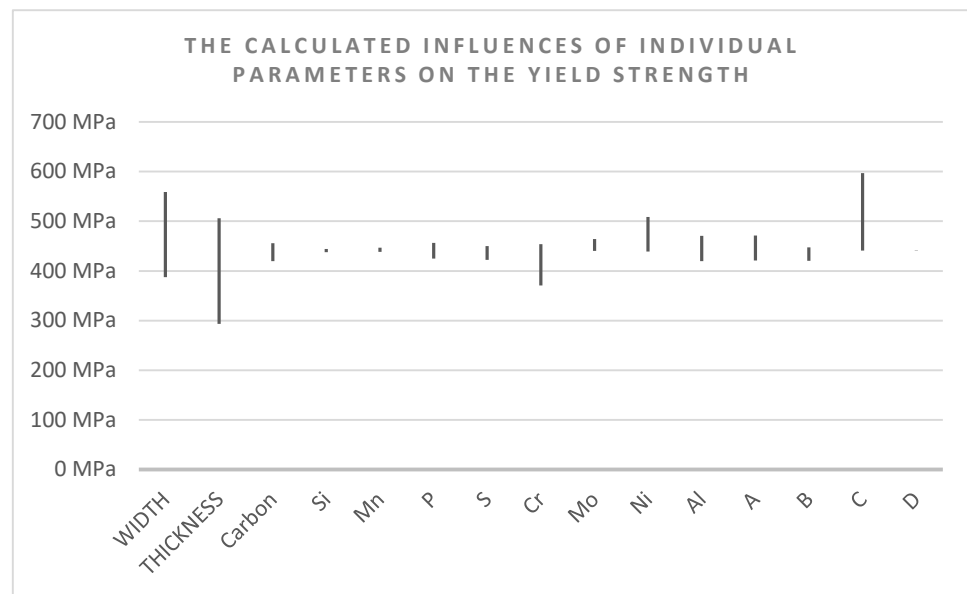


Figure 3. The calculated influences of individual parameters on the yield strength while separately changing individual parameter within the individual parameter range.

The next model significantly predicts the percentage elongation ($p < 0.05$, ANOVA) but only 7.55% of total variances can be explained by independent variables variances (R-square). Significantly influential parameters ($p > 0.05$) are hot rolled bar width (WIDTH) and thickness (THICKNESS) and chromium content (Cr).

$$\begin{aligned}
 \text{Elongation} = & 0.039 \cdot WIDTH - 0.024 \cdot THICKNESS + 1.13 \cdot Carbon + 2.05 \cdot Si + 0.32 \\
 & \cdot Mn + 138.87 \cdot P - 9.87 \cdot S + 1.22 \cdot Cr - 6.62 \cdot Mo - 2.21 \cdot Ni \\
 & + 112.86 \cdot Al - 0.43 \cdot A + 0.89 \cdot B - 5.50 \cdot C + 0.33 \cdot D + 14.12
 \end{aligned} \quad (4)$$

The average relative deviation from experimental data is 25.47%.

Moreover, the influences of individual parameters on the percentage elongation while separately changing individual parameter within the individual parameter range were calculated (Figure 4). It is possible to conclude that according to linear regression results the most influential are alumina and silicate type of inclusions (C).

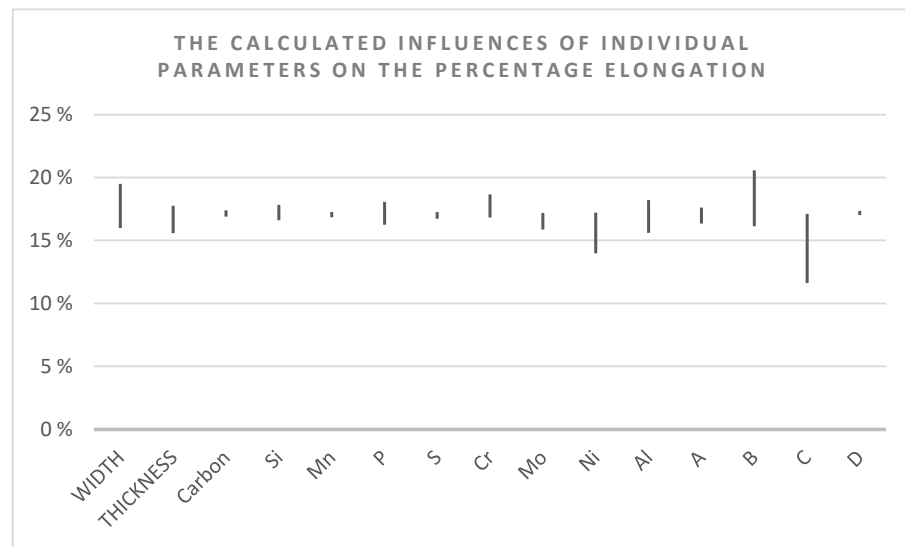


Figure 4. The calculated influences of individual parameters on the percentage elongation while separately changing individual parameter within the individual parameter range.

The next model significantly predicts the percentage reduction area ($p < 0.05$, ANOVA) but only 14.40% of total variances can be explained by independent variables variances (R-square). Significantly influential parameters ($p > 0.05$) are hot rolled bar width (WIDTH) and thickness (THICKNESS), aluminium content (Al) and aluminium type of inclusions (B).

$$\begin{aligned} \text{Reduction} = & 0.49 \cdot \text{WIDTH} - 0.39 \cdot \text{THICKNESS} + 8.89 \cdot \text{Carbon} + 4.93 \cdot \text{Si} - 2.02 \cdot \text{Mn} \\ & + 387.25 \cdot \text{P} + 144.12 \cdot \text{S} + 4.67 \cdot \text{Cr} - 53.03 \cdot \text{Mo} + 20.40 \cdot \text{Ni} \\ & + 603.89 \cdot \text{Al} + 3.61 \cdot \text{A} + 2.25 \cdot \text{B} + 41.93 \cdot \text{C} + 3.51 \cdot \text{D} + 13.47 \end{aligned} \quad (5)$$

The average relative deviation from experimental data is 31.84%.

Moreover, the influences of individual parameters on the percentage reduction area while separately changing individual parameter within the individual parameter range were calculated (Figure 5). It is possible to conclude that according to linear regression results the most influential are hot rolled bar width (WIDTH) and thickness (THICKNESS), nickel content, and silicate type of inclusions (C).

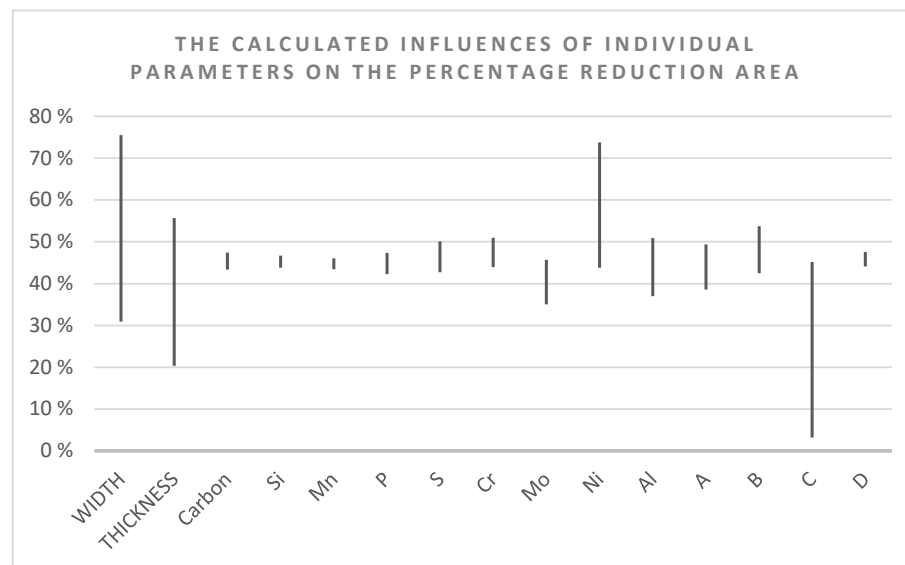


Figure 5. The calculated influences of individual parameters on the percentage reduction area while separately changing individual parameter within the individual parameter range.

3.2. Modeling of Tensile, Yield Strength, Percentage Elongation and Reduction Area Using Genetic Programming

In genetic programming, which is one of the most general evolutionary optimization methods, the organisms that undergo adaptation are in fact mathematical expressions (models) [20]. These models consist of the selected function (e.g., basic arithmetical functions) and terminal genes (e.g., independent input parameters, and random floating-point constants). Typical function genes are: addition (+), subtraction (-), multiplication (*) and division (/), and terminal genes (e.g., x, y, z).

Random computer programs for calculating various forms and lengths are generated by means of the selected genes at the beginning of the simulated evolution. The varying of the computer programs is carried out by means of genetic operations (e.g., crossover, mutation) during several iterations, called generations. After the completion of the variation of the computer programs, a new generation is obtained. Each result obtained from an individual program from a generation is evaluated with a comparison to the experimental data. The process of changing and evaluating organisms is repeated until the termination criterion of the process is fulfilled. Figure 6 shows the pseudo code for genetic programming system.

```

begin
  t = 0
  initialize population(t)
  evaluate population(t)
  while (not termination condition) do
    t = t+1
    change population(t) by applying genetic operators
    evaluate population(t)
  end
  output of results
end

```

Figure 6. The pseudo code for genetic programming system.

In-house genetic programming system [21–24], programmed using AutoLISP, which is integrated into AutoCAD (AutoCAD Release 14, Autodesk, San Rafael, California, USA) (i.e., commercial computer-aided design software), was used. Its settings were:

- size of the population of organisms: 1000,
- maximum number of generations: 100,
- reproduction probability: 0.4,
- crossover probability: 0.6,
- maximum permissible depth in the creation of the population: 5,
- maximum permissible depth after the operation of crossover of two organisms: 30 and
- smallest permissible depth of organisms in generating new organisms: 2.

Genetic operations of reproduction and crossover were used. For selection of organisms the tournament method with tournament size 7 was used.

The AutoLISP based in-house genetic programming system was run 100 times in order to develop 100 independent civilizations for each individual mechanical property. Each run for tensile, yield strength, percentage elongation, and reduction area lasted approximately 16 min and 57 s, 14 min and 23 s, 17 min and 27 s, 9 min, and 8 s on an I7 Intel processor with 8 GB of RAM, respectively.

The best mathematical model for prediction of tensile strength obtained from 100 runs of genetic programming system is:

$$\begin{aligned}
 R_m = & (A + D)(-69.4449 - D + \text{WIDTH}) - \\
 & D \left(\left(\frac{8.33336(-8.33336 + A) + (-\text{Carbon} + D)(8.33336(A + D) - \text{THICKNESS} + \text{WIDTH})}{(-69.4449 + \text{WIDTH})} \right) \right. \\
 & - (A + \text{Mn}) \left(-69.4449 + \text{WIDTH} \right. \\
 & \left. - \frac{A + C + 10.3334D + \text{THICKNESS}}{(8.33336C + D)(C + \text{Carbon} + D + \text{THICKNESS}) + (A + D)} \right. \\
 & \left. - \frac{(-69.4449 + 10.3334D + \text{THICKNESS})}{D} + \text{WIDTH} \right) \\
 & - \text{Mn} \left(\frac{-69.4449 - D + \text{WIDTH} - \text{THICKNESS} + (A + C)^2(C - 8.33336D + \text{THICKNESS}) - \text{WIDTH} + (D + 8.33336D(-C + D)) \left(-69.4449 - \frac{C}{D + \text{THICKNESS}} + \text{WIDTH} \right)}{\text{WIDTH}} \right) \\
 & + D \left(D - \frac{C + \text{THICKNESS} + (A + D)}{C} \right)
 \end{aligned} \tag{6}$$

Its average relative deviation from experimental data is 15.73%.

Similarly, as with linear regression, individual parameters influence tensile strength while separately changing individual parameters within the individual parameter range were calculated also (Figure 7). It is possible to conclude that according to genetic programming results, the most influential are silicate type inclusions (C).

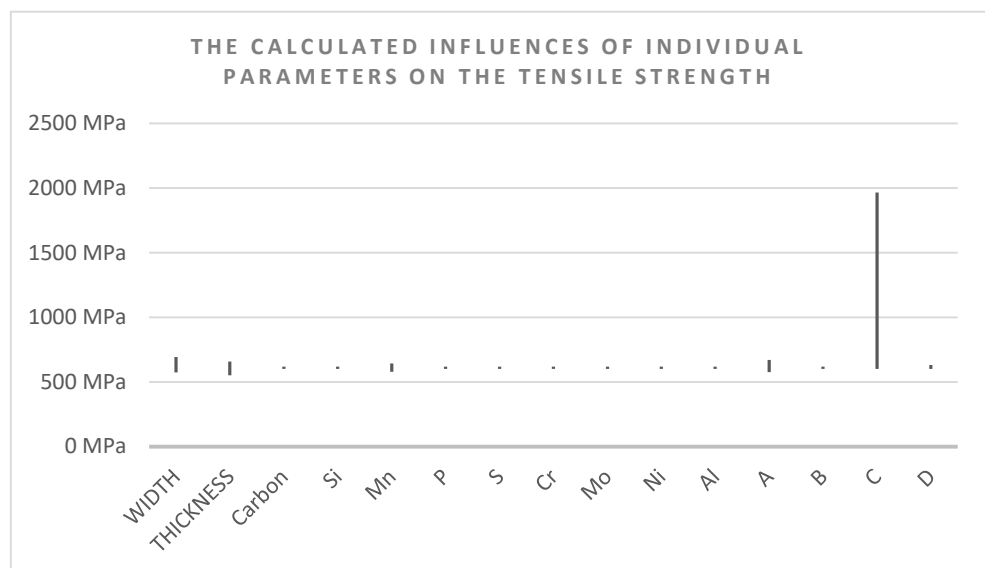


Figure 7. The calculated influences of individual parameters on the tensile strength while separately changing individual parameter within the individual parameter range.

The best mathematical model for prediction of yield strength obtained from 100 runs of genetic programming system is:

$Rp0.2$

$$= \left(\begin{array}{l} 101.14 + 20A + 3Mo + \frac{3.P}{Mo} + \frac{(67.4269 + 5A + Mo + P - WIDTH)}{A + 2Mo} - \\ 6WIDTH + 6.74269 \left(33.7134 - A - Mo + \frac{(14.4854 + A + Carbon)}{AWIDTH} + WIDTH \right) + \\ c \left(20.2281 - 2Mo - \frac{1.P}{Mo} + \frac{1.(67.4269 + 5A + Mo + P - WIDTH)}{A} + 3WIDTH \right) \end{array} \right)^2 THIC \quad (7)$$

Its average relative deviation from experimental data is 15.24%.

Moreover, the influences of individual parameters on the yield strength while separately changing individual parameter within the individual parameter range were calculated (Figure 8). It is possible to conclude that according to genetic programming results, the most influential are silicate type of inclusions (C).

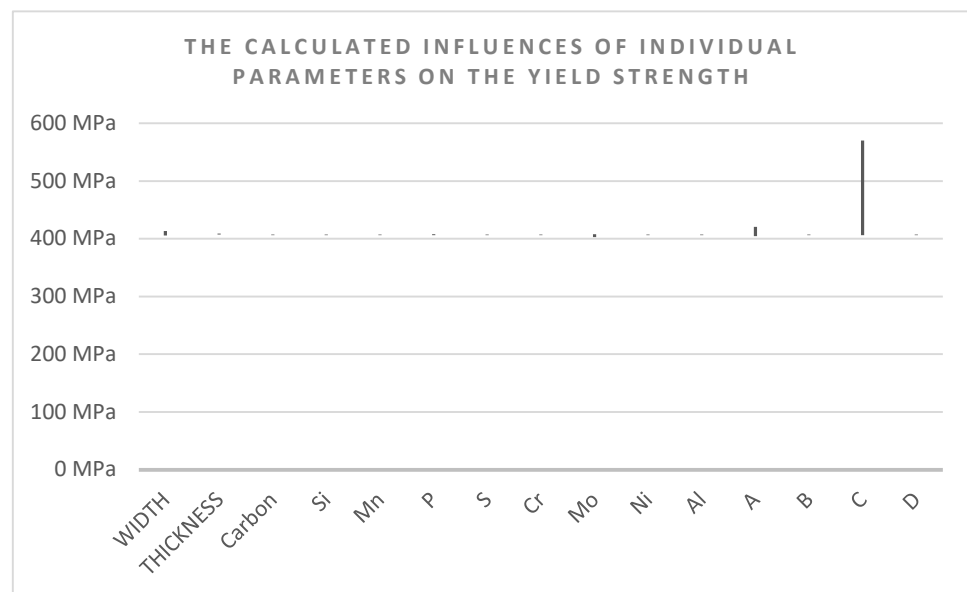


Figure 8. The calculated influences of individual parameters on the yield strength while separately changing individual parameter within the individual parameter range.

The best mathematical model for prediction of percentage elongation obtained from 100 runs of genetic programming system is:

$$\begin{aligned}
 \text{Elongation} = & -5.5889 + 3\text{Al} + \frac{\text{THICKNESS}}{-5.5889 - \text{Al}} - \\
 & \frac{\text{THICKNESS}}{5.5889 - \text{Al}} - \frac{\text{THICKNESS}}{5.5889 - \text{Al}} + \frac{\text{THICKNESS}}{-5.5889 - \text{WIDTH} + \text{Carbon}} - \\
 & \frac{\text{THICKNESS}}{5.5889 + \text{Al}} - \frac{\text{THICKNESS}}{5.5889 - \text{Al}} - \frac{2\text{THICKNESS}}{5.5889 - \text{WIDTH}} + \frac{\text{THICKNESS}}{\text{WIDTH}} + \frac{\text{THICKNESS}}{5.5889 - \text{WIDTH}} - \text{WIDTH} \\
 & \frac{5.5889 - \text{Al} - \frac{\text{THICKNESS}}{5.5889 - \text{Al}} + \text{Carbon} + \text{WIDTH}}{5.5889 - \text{Al} - \frac{\text{THICKNESS}}{5.5889 - \text{S}} + \frac{\text{THICKNESS}}{5.5889 - \text{WIDTH}}} \\
 & \frac{-5.5889 - 0.178926\text{THICKNESS} + \frac{\text{THICKNESS}}{5.5889 - \text{Al}} - \frac{2\text{THICKNESS}}{5.5889 - \text{WIDTH}}}{-5.5889 + \text{Al} - \text{THICKNESS} + \frac{\text{THICKNESS}}{5.5889 - \frac{\text{THICKNESS}}{5.5889 - \text{Al}}} + \frac{\text{THICKNESS}}{5.5889 - \text{WIDTH}} - \text{WIDTH}} + \text{WID} \quad (8)
 \end{aligned}$$

Its average relative deviation from experimental data is 22.72%.

Moreover, the influences of individual parameters on the percentage elongation while separately changing individual parameter within the individual parameter range were calculated (Figure 9). It is possible to conclude that according to genetic programming results the most influential are silicon content, sulfide (A) and alumina (B) type inclusions.

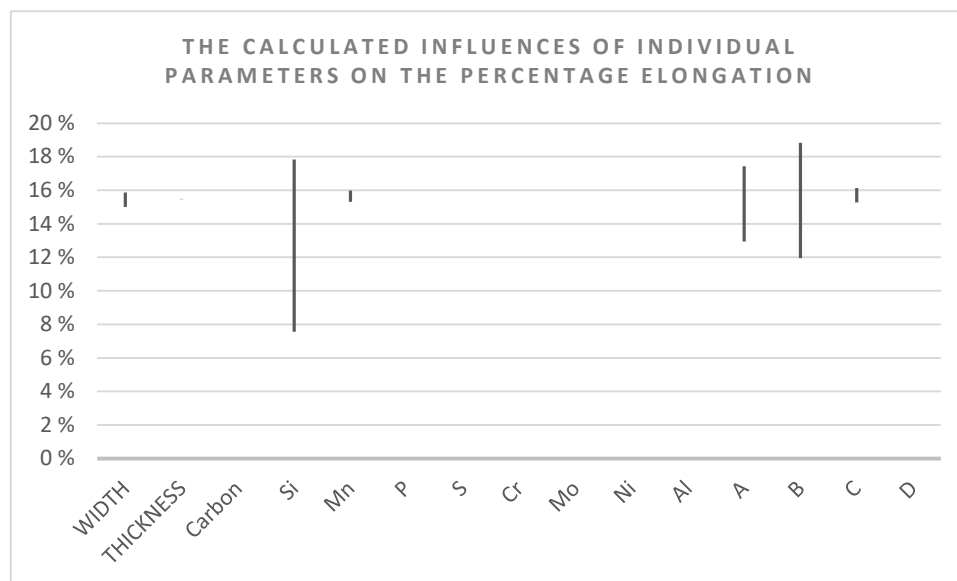


Figure 9. The calculated influences of individual parameters on the percentage elongation while separately changing individual parameter within the individual parameter range.

The best mathematical model for prediction of percentage reduction area obtained from 100 runs of genetic programming system is:

$$\begin{aligned}
 \text{Reduction} = & 15.6976 - A + B + \frac{C}{-A + Mn + ASi + \frac{Si}{WIDTH}} - \\
 & \frac{\left(10.1939 - B - ASi - Si^2 - \frac{(ASi + Si^2)}{A} - SiWIDTH \right)}{\left(\frac{5.09697 + B - C + Mn - MnSi -}{A} \right)} - \\
 & \frac{\left(\frac{5.09697 - 2A + Mn - MnSi - Si(5.09697 - 2ASi)}{-A - B - Carbon + Mn + ASi + \frac{Si}{WIDTH}} \right) + WIDTH}{A} + \text{THICKNESS} \quad (9) \\
 & \frac{5.09697 - A + B + Mn - Si \left(\frac{5.09697 - A + B + Mn - MnSi -}{A} \right) - \frac{C}{-A + Mn + \frac{Si}{WIDTH}} + \frac{Si}{WIDTH}}{\left(\frac{5.09697 - 2A + Mn - MnSi - Si(5.09697 - 2ASi)}{-A - B - Carbon + 2Mn - \frac{Si}{A} - ASi - MnSi - SiWIDTH} \right) + WIDTH} - \\
 & \frac{Si(-A + Mn + Si(A - Mn + MnSi + Si(5.09697 - 2ASi))) + WIDTH}{Si(5.09697 - A + B - Carbon + 2Mn - \frac{Si}{A} - ASi - MnSi - SiWIDTH)}
 \end{aligned}$$

Its average relative deviation from experimental data is 28.16%.

Moreover, the influences of individual parameters on the percentage reduction area while separately changing individual parameter within the individual parameter range were calculated (Figure 10). It is possible to conclude that according to genetic programming results, the most influential are hot rolled bar width (WIDTH) and thickness (THICKNESS) and aluminum content (Al).

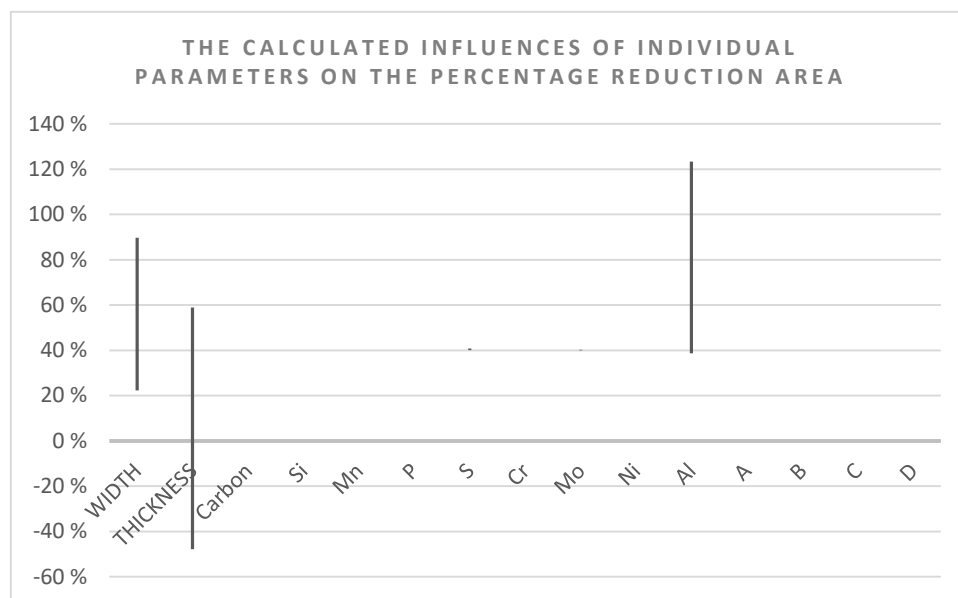


Figure 10. The calculated influences of individual parameters on the percentage reduction area while separately changing individual parameter within the individual parameter range.

4. Modeling Results and Validation

The 30MnVS6 steel grade is used in automotive industry for highly stressed parts because the mechanical properties of forged parts using micro-alloyed steels are obtained with the grain refinement using vanadium addition. Consequently, the precipitation hardening enables the elimination of the additional heat treatment processes [25,26]. It is

also the third best-selling steel grade at In Štore Steel Ltd., which is used by the final user in rolled condition.

Based on linear regression and genetic programming results, it is possible to conclude that the hot rolled bar width (WIDTH) and thickness (THICKNESS) and silicate type inclusions (C) are most influential. Unfortunately, the geometrical features are defined by the final customer and only the content of silicate type of inclusions could be changed. Based on modeling results (linear regression and genetic programming) the tensile strength decreases with increasing content of silicate type of inclusions. Deductively, we can conclude that by increasing of the silicon content, we increase the content of silicate type inclusions (C).

In the period from January 2022 to April 2022 five successively cast batches of 30MnVS6 were produced with statistically significant reduction of content of silicon (t -test, $p < 0.05$). The content of silicate type inclusions (Kruskal-Wallis test, $p < 0,05$), yield, and tensile strength also changed statistically significantly (t -test, $p < 0.05$). The average yield and tensile strength increased from 458.5 MPa to 525.4 MPa and from 672.7 MPa to 754.0 MPa, respectively. It is necessary to emphasize that there were no statistically significant changes in other monitored parameters.

The chemical composition of and severity numbers for inclusions determined according to standard ASTM E45, method A and geometry and mechanical properties for five successively cast batches of 30MnVS6 with a statistically significant reduction of the content of silicon are presented in Tables 3 and 4, respectively.

Table 3. The chemical composition of five successively cast batches of 30MnVS6 and severity numbers for inclusions determined according to standard ASTM E45, method A.

| Batch Number | wt % C | wt % Si | wt % Mn | wt % P | wt % S | wt % Cr | wt % Mo | wt % Ni | wt % Al | Severity Number A | Severity Number B | Severity Number C | Severity Number D |
|--------------|--------|---------|---------|--------|--------|---------|---------|---------|---------|-------------------|-------------------|-------------------|-------------------|
| 1 | 0.28 | 0.65 | 1.44 | 0.013 | 0.03 | 0.14 | 0.03 | 0.08 | 0.016 | 0.5 | 1.5 | 1.5 | 0 |
| 2 | 0.27 | 0.61 | 1.41 | 0.01 | 0.022 | 0.19 | 0.04 | 0.11 | 0.015 | 0.5 | 1.5 | 1.5 | 0 |
| 3 | 0.29 | 0.65 | 1.43 | 0.013 | 0.029 | 0.15 | 0.03 | 0.12 | 0.017 | 0.5 | 2.5 | 1.5 | 0 |
| 4 | 0.3 | 0.65 | 1.49 | 0.013 | 0.026 | 0.2 | 0.03 | 0.12 | 0.019 | 0.5 | 2 | 1.5 | 0 |
| 5 | 0.27 | 0.66 | 1.42 | 0.012 | 0.028 | 0.12 | 0.03 | 0.08 | 0.014 | 0.5 | 2 | 3 | 0 |

Table 4. The geometry and mechanical properties for five successively cast batches of 30MnVS6 with statistically significant reduction of content of silicon.

| Batch Number | Hot Rolled Bar Width [mm] | Hot Rolled Bar Thickness [mm] | Tensile Strength [MPa] | Yield Strength [MPa] | Percentage Elongation [%] | Percentage Reduction [%] |
|--------------|---------------------------|-------------------------------|------------------------|----------------------|---------------------------|--------------------------|
| 1 | 60 | 60 | 735 | 512 | 18.9 | 50.0 |
| 2 | 60 | 60 | 727 | 498 | 17.8 | 47.7 |
| 3 | 30 | 30 | 783 | 560 | 11.4 | 38.1 |
| 4 | 60 | 60 | 767 | 534 | 14 | 51.4 |
| 5 | 32 | 32 | 758 | 523 | 14.7 | 35.2 |

In addition, the developed linear regression and genetic programming model were used for the prediction of mechanical properties of five successively cast batches of 30MnVS6 with statistically significant reduction of content of silicon.

The average relative deviation from experimental data of the linear regression model for tensile strength, yield strength, percentage elongation, and percentage reduction area is 34.60%, 45.13%, 45.16%, and 128.42%, respectively.

The average relative deviation from experimental data of the genetic programming model for tensile strength, yield strength, percentage elongation, and percentage reduction area is 18.67%, 9.47%, 24.21%, and 14.97%, respectively, which is significantly better than when using the model linear regressions.

5. Conclusions

In this paper, the influence of non-metallic inclusions on mechanical properties obtained by tensile testing was studied. From January 2016 to December 2021, all available tensile strength data (472 cases–472 test pieces) of 17 low alloy steel grades, which were ordered and used by the final user in rolled condition, were gathered.

Samples were obtained from rolled bars with diameter from 18 mm to 110 mm and flat bars with thickness from 8 mm to 73 mm and width from 45 mm to 200 mm from the middle billet of the rolling lot.

Based on the geometry of rolled bars, selected chemical composition, and average size of worst fields non-metallic inclusions (sulfur, silicate, aluminium and globular oxides), determined according to ASTM E45, method A, several models for tensile strength, yield strength, percentage elongation, and percentage reduction area were obtained using linear regression and genetic programming.

According to linear regression and genetic programming results, it is possible to conclude that the hot rolled bar width and thickness and silicate type inclusions are most influential. Unfortunately, the geometrical features are defined by the final customer and only the content of silicate type of inclusions could be changed. Based on modeling results (linear regression and genetic programming), the tensile strength decreases with an increasing content of silicate type inclusions. Deductively, we can conclude that by increasing of the silicon content, we increase the content of silicate type inclusions.

Based on modeling results in the period from January 2022 to April 2022, five successively cast batches of 30MnVS6 were produced with a statistically significant reduction of the content of silicon (*t*-test, $p < 0.05$). The content of silicate type inclusions (Kruskal–Wallis test, $p < 0.05$), yield, and tensile strength also changed statistically significantly (*t*-test, $p < 0.05$). The average yield and tensile strength increased from 458.5 MPa to 525.4 MPa and from 672.7 MPa to 754.0 MPa, respectively. It is necessary to emphasize that there were no statistically significant changes in other monitored parameters.

The average relative deviation from experimental data of the linear regression model for tensile strength, yield strength, percentage elongation, and percentage reduction area for five successively cast batches of 30MnVS6 are 34.60%, 45.13%, 45.16%, and 128.42%, respectively.

The average relative deviation from experimental data of the genetic programming model for tensile strength, yield strength, percentage elongation, and percentage reduction area for five successively cast batches of 30MnVS6 is 18.67%, 9.47%, 24.21%, and 14.97%, respectively, which is significantly better than when using the model linear regressions.

In the future, the focus will be on variously heat treated samples and more than 50 numbers different steel grades which are produced in the steel plant. Moreover, the results of Charpy impact testing will be taken into account. In particular, a deep investigation of the mechanisms involved should be considered.

Author Contributions: Conceptualization, M.K. and U.Ž.; methodology, M.K. and U.Ž.; software, M.K.; validation, M.K.; formal analysis, M.K. and U.Ž.; investigation, M.K.; resources, M.K. and U.Ž.; data curation, M.K.; writing—original draft preparation, M.K. and U.Ž.; writing—review and editing, M.K. and U.Ž.; visualization, M.K.; supervision, M.K. and U.Ž. All authors have read and agreed to the published version of the manuscript.

Funding: This research received no external funding.

Data Availability Statement: The data are not publicly available due to business confidentiality.

Conflicts of Interest: The authors declare no conflict of interest.

References

1. Qiu, G.-X.; Wei, X.-L.; Bai, C.; Miao, D.-J.; Cao, L.; Li, X.-M. Inclusion and mechanical properties of ODS-RAFM steels with Y, Ti, and Zr fabricated by melting. *Nucl. Eng. Technol.* **2022**, *54*, 2376–2385. <https://doi.org/10.1016/j.net.2022.01.030>.
2. Gong, W.; Jiang, Z.; Zhang, L.; Chen, C.; Dong, Y. Influence of Mg addition on inclusions and mechanical properties of Cr12Mo1V1 steel under high pressure. *Mater. Sci. Eng. A* **2020**, *791*, 139410. <https://doi.org/10.1016/j.msea.2020.139410>.
3. Arreola-Herrera, R.; Cruz-Ramírez, A.; Rivera-Salinas, J.E.; Romero-Serrano, A.; Sánchez-Alvarado, R.G. The effect of non-metallic inclusions on the mechanical properties of 32 CDV 13 steel and their mechanical stress analysis by numerical simulation. *Theor. Appl. Fract. Mech.* **2018**, *94*, 134–146. <https://doi.org/10.1016/j.tafmec.2018.01.013>.
4. Liu, S.; Huang, Q.; Li, C.; Huang, B. Influence of non-metal inclusions on mechanical properties of CLAM steel. *Fusion Eng. Des.* **2009**, *84*, 1214–1218. <https://doi.org/10.1016/j.fusengdes.2008.12.037>.
5. Liu, X.; Yang, J.; Zhang, F.; Fu, X.; Li, H.; Yang, C. Experimental and DFT study on cerium inclusions in clean steels. *J. Rare Earths* **2021**, *39*, 477–486. <https://doi.org/10.1016/j.jre.2020.07.021>.
6. Wu, M.; Fang, W.; Chen, R.-M.; Jiang, B.; Wang, H.-B.; Liu, Y.-Z.; Liang, H.-L. Mechanical anisotropy and local ductility in transverse tensile deformation in hot rolled steels: The role of MnS inclusions. *Mater. Sci. Eng. A* **2019**, *744*, 324–334. <https://doi.org/10.1016/j.msea.2018.12.026>.
7. Qiu, G.-X.; Zhan, D.-P.; Cao, L.; Zhang, H.-S. Effect of zirconium on inclusions and mechanical properties of China low activation martensitic steel. *J. Iron Steel Res. Int.* **2021**, *28*, 1168–1179. <https://doi.org/10.1007/s42243-021-00572-8>.
8. Aydın, E.; Arısoy, C.F.; Sesen, M.K. The Effect of Manganese Sulfide Inclusions and Zirconium Additions on the Mechanical Properties of Heavy Section Cast Steel. *Int. J. Met.* **2018**, *12*, 383–395. <https://doi.org/10.1007/s40962-017-0175-2>.
9. Lu, J.; Cheng, G.; Che, J.; Wang, L.; Xiong, G. Effect of Oxides on Characteristics of MnS and Transverse Mechanical Properties in Commercial Al-Killed Non-Quenched and Tempered Steel. *Met. Mater. Int.* **2019**, *25*, 473–486. <https://doi.org/10.1007/s12540-018-0191-7>.
10. Maisuradze, M.V.; Björk, T. Microstructure and Mechanical Properties of Calcium Treated 42CRMO4 Steel with Improved Machinability. *Trans. Indian Inst. Met.* **2022**, *75*, 681–690. <https://doi.org/10.1007/s12666-021-02463-8>.
11. Qiao, X.; Han, X.; He, Z.; Zhuang, Z.; Yang, X.; Mao, F. Effect of cerium addition on microstructure and mechanical properties of as-cast high grade knives steel. *J. Iron Steel Res. Int.* **2022**, preprint. <https://doi.org/10.1007/s42243-022-00798-0>.
12. Qiu, G.; Zhan, D.; Li, C.; Yang, Y.; Qi, M.; Jiang, Z.; Zhang, H. Effects of Yttrium and Heat Treatment on the Microstructure and Mechanical Properties of CLAM Steel. *J. Mater. Eng. Perform.* **2020**, *29*, 42–52. <https://doi.org/10.1007/s11665-020-04574-7>.
13. Brytan, Z.; Król, M.; Benedyk, M.; Pakieła, W.; Tański, T.; Dagnaw, M.J.; Snopiński, P.; Pagáč, M.; Czech, A. Microstructural and Mechanical Properties of Novel Co-Free Maraging Steel M789 Prepared by Additive Manufacturing. *Materials* **2022**, *15*, 1734. <https://doi.org/10.3390/ma15051734>.
14. Liu, J.; Liu, D.; Zuo, X.; Liu, L.; Yan, Q. Influence of TiN Inclusions and Segregation on the Delayed Cracking in NM450 Wear-Resistant Steel. *Metals* **2021**, *12*, 21. <https://doi.org/10.3390/met12010021>.
15. Jonšta, P.; Jonšta, Z.; Brožová, S.; Ingaldi, M.; Pietraszek, J.; Klimecka-Tatar, D. The Effect of Rare Earth Metals Alloying on the Internal Quality of Industrially Produced Heavy Steel Forgings. *Materials* **2021**, *14*, 5160. <https://doi.org/10.3390/ma14185160>.
16. Gong, W.; Wang, P.; Zhang, L.; Jiang, Z. Effects of Ce on Microstructure and Mechanical Properties of LDX2101 Duplex Stainless Steel. *Metals* **2020**, *10*, 1233. <https://doi.org/10.3390/met10091233>.
17. Chen, R.; Wang, Z.; He, J.; Zhu, F.; Li, C. Effects of Rare Earth Elements on Microstructure and Mechanical Properties of H13 Die Steel. *Metals* **2020**, *10*, 918. <https://doi.org/10.3390/met10070918>.
18. Ali, M.; Nyo, T.; Kaijalainen, A.; Javaheri, V.; Tervo, H.; Hannula, J.; Somani, M.; Kömi, J. Incompatible effects of B and B + Nb additions and inclusions' characteristics on the microstructures and mechanical properties of low-carbon steels. *Mater. Sci. Eng. A* **2021**, *819*, 141453. <https://doi.org/10.1016/j.msea.2021.141453>.
19. Gupta, A.; Goyal, S.; Padmanabhan, K.A.; Singh, A.K. Inclusions in steel: Micro–macro modelling approach to analyse the effects of inclusions on the properties of steel. *Int. J. Adv. Manuf. Technol.* **2015**, *77*, 565–572. <https://doi.org/10.1007/s00170-014-6464-5>.
20. Koza, J.R. *Genetic Programming: On the Programming of Computers by Means of Natural Selection*; MIT Press: Cambridge, MA, USA, 1992.
21. Kovačič, M.; Župerl, U. Genetic programming in the steelmaking industry. *Genet. Program. Evolvable Mach.* **2020**, *21*, 99–128. <https://doi.org/10.1007/s10710-020-09382-5>.
22. Babič, M.; Marinković, D.; Kovačič, M.; Šter, B.; Cali, M. A New Method of Quantifying the Complexity of Fractal Networks. *Fractal Fract.* **2022**, *6*, 282. <https://doi.org/10.3390/fractalfract6060282>.
23. Kovačič, M.; Lešer, B.; Brezocnik, M. Modelling and optimization of sulfur addition during 70MnVS4 steelmaking: An industrial case study. *Adv. Prod. Eng. Manag.* **2021**, *16*, 253–261. <https://doi.org/10.14743/apem2021.2.398>.
24. Kovačič, M.; Salihu, S.; Gantar, G.; Župerl, U. Modeling and Optimization of Steel Machinability with Genetic Programming: Industrial Study. *Metals* **2021**, *11*, 426. <https://doi.org/10.3390/met11030426>.
25. Kovačič, M.; Novak, D. Prediction of the chemical non-homogeneity of 30MnVS6 billets with genetic programming. *Mater. Teh.* **2016**, *50*, 69–74. <https://doi.org/10.17222/mit.2014.280>.
26. Da Maia, B.I.; Futami, A.H.; De Oliveira, M.A. Vanadium Alloy Steel DIN 30MnVS6 Applied in Cold Forging Process. *ISIJ Int.* **2018**, *58*, 2318–2322. <https://doi.org/10.2355/isijinternational.ISIJINT-2018-342>.